

Measurements of the Anisotropic Viscous and Elastic Properties of Lyotropic Polymer Nematics

BY ROBERT B. MEYER,* FRANKLIN LONBERG, VICTOR TARATUTA, SETH FRADEN,
SIN-DOO LEE AND ALAN J. HURD

The Martin Fisher School of Physics, Brandeis University, Waltham,
Massachusetts 02254, U.S.A.

Received 9th May, 1985

We summarize the current status of our studies of the macroscopic linear mechanical properties of nematic liquid crystals formed from solutions of rigid or semirigid rod-like polymers. The polymer system we have studied is a racemic mixture of poly(benzyl glutamate) dissolved in a mixture of dioxane and methylene chloride. We have also studied nematics formed from colloidal suspensions of tobacco mosaic virus which may be viewed as an ideal model system representing a rigid-rod polymer solution. We review briefly the current theoretical understanding of the elastic and viscous parameters characterizing a nematic. Then we discuss our experiments, both Frederiks-transition studies and quasielastic Rayleigh scattering. The Frederiks transition in its well known simple forms is not easily utilized in these systems, mainly because of the intervention of a number of phenomena not normally encountered in low-molecular-weight liquid crystals. However, these phenomena have been analysed theoretically and can be used to extract information on elastic and viscous properties. Quasielastic Rayleigh scattering on well oriented single crystals has proved to be an excellent technique for measuring ratios of elastic and viscous parameters. We describe the scattering geometries we have used and our results.

An important goal in the study of polymer nematic liquid crystals is the complete understanding of their mechanical properties. We have undertaken a program of research concerning the linear mechanical properties of systems of rod-like or semiflexible polymers that form nematic phases in solution. These form a fairly simple limiting case for two reasons. First, fairly simple theoretical ideas based on a dilute-solution limit might be almost correct. Secondly, the preparation of and experimentation on such samples is easier than the study of melts in a number of ways. In particular, we have studied racemic mixtures of poly(benzyl glutamate) (PBG) in a solvent which is a mixture of dioxane and methylene chloride, to suppress any remaining cholesteric helicity.¹ We have also studied the nematic phase of colloidal suspensions of tobacco mosaic virus (TMV), which in this context may be thought of as an ideal model of a rigid-rod polymer solution.

The experimental methods we have used include the Frederiks transition and quasielastic Rayleigh scattering. The first of these has been used extensively in the study of low-molecular-weight nematics to determine their elastic constants and viscosities.² The second has been used in the study of nematics,³ but it presents some serious technical problems for the routine determination of mechanical properties owing to the large birefringence of the nematic phase.⁴ However, in our materials, which have very low birefringence, this technique works very well. Rather, it is the Frederiks transition that presents difficulties of various kinds. Several new phenomena are encountered when trying to study the Frederiks transition which prevent the straightforward extraction of information from this experiment.

However, these new phenomena are very interesting in their own right, and in the light of theoretical analysis they provide new ways of studying the mechanical properties of polymer nematics.

In the following sections we first review our understanding of the theory of the elastic and viscous properties of nematics composed of rigid rods or semirigid chains, and then we discuss our experimental findings.

THEORY

The starting point for theory of lyotropic nematics is the hard-rod model first investigated by Onsager.⁵ This views the interaction between particles as arising entirely out of the excluded-volume effect. The appearance of the nematic phase is the result of maximizing the entropy of the system; in the nematic phase, rotational entropy is sacrificed to increase the configurational entropy of the molecular positions. In the approximation used by Onsager all that matters are two-body interactions, which are treated in a mean-field approximation. At the level of this approximation one can solve the equations describing the nematic-isotropic phase equilibrium, and compute the orientational distribution function for the molecules in the nematic phase. From this distribution function, and still at the level of approximation using two-body interactions in a mean-field calculation, one can compute the elastic constants⁶ and viscosities⁷ of the nematic phase. We have carried out these computations as a starting point for comparison of experimental results with theory.⁸ The results are summarized in table 1.

For describing TMV, the theory at the Onsager level might be at least a good starting point. However, for longer and more flexible particles, such as PBG, and surely for even longer and much more flexible particles, such as many other currently studied polymers, or for more concentrated solutions and melts, other theoretical ideas are needed. Here we consider only the possibility of semiflexible particles, which are non-rigid but are still fully extended in the nematic phase.

In the Onsager picture of the elastic constants, all that is taken into account is the change in the two-particle excluded volume produced by spatial distortions of the director field. All the elastic constants scale with the square of the volume fraction of polymer in solution and the square of the length-to-diameter ratio. For highly oriented states of the nematic, this theory predicts that the bend elastic constant will be large, while those for splay and twist will be small, since bend always increases interference effects, while splay and twist do so only as second-order effects. Moreover, the bend elastic constant increases roughly linearly with order parameter in the range of experimentally reasonable order parameters, diverging to infinity at perfect order. This is a consequence of the singular form of the two-body excluded-volume function, which varies as the absolute value of the sine of the angle between two rods. These are interesting predictions to check.

Beyond the Onsager picture of the elastic constants there are two ideas for longer, more flexible chains.⁹ First, the splay elastic constant has a component arising from a single particle contribution to the entropy. Splay requires concentrating like ends of the chains ('top' or 'bottom' ends), which reduces their entropy. This contribution exists for hard rods and for more flexible chains, and increases linearly with chain length and concentration. It is larger than the two-particle interference contribution to the splay elastic constant. For flexible chains the bend elastic constant is limited by the flexibility of the chains. It no longer increases with chain length, and varies linearly with concentration rather than quadratically. It simply reflects the energy per unit volume needed to bend the chains. Thus for

Table 1. Elastic constants and viscosities of the nematic phases^a

	hard-rod theory			TMV	PBG
	$S = 0.7$	$S = 0.8$	$S = 0.9$		
	elastic moduli				
K_1	1.8	2.1	3.3		4.1
K_2	0.6	0.69	1.1		0.36
K_3	8.0	14.0	43.0		4.7
K_1/K_2	3	3	3	2.5	11.4
K_3/K_2	13	21	42	42.5	13.0
	viscosities				
γ_1					34.7
η_b					0.16
η_c					35.1
$ \alpha_3 $					≤ 0.16
$ \alpha_2 $					34.8
η_a/η_c	0.054	0.034	0.017	0.044	
η_b/η_c	0.032	0.016	0.004	0.015	0.0046
γ_1/η_b	34.8	69.6	240	63.3	220
γ_1/η_c	1.13	1.11	1.06	0.95	1.0
ν_1/η_c	0.15	0.11	0.06	0.21	

^a The notation follows P. G. deGennes, *The Physics of Liquid Crystals* (Clarendon Press, Oxford, 1974). S is the nematic order parameter. The units for K_i are 10^{-7} dyn, assuming a diameter for PBG of 15 Å. The units for the viscosities are poise. The accuracy of the PBG measurements is $\pm 7\%$.

fully extended but non-rigid chains, the ratio of splay to bend elastic constants should be relatively large, independent of concentration and proportional to chain length, rather different from the hard-rod limit, in which this ratio would be small and decreasing with increasing chain length.

The hard-rod picture qualitatively predicts that certain viscosities grow very large with molecular length and increasing order parameter, while others remain small.⁷ All the viscosities are proportional to a fundamental rotational viscosity for a single particle which depends on its shape and the solvent viscosity. For semiflexible chains, the same qualitative conclusions apply. The ability of semiflexible chains to wrap rather gently around one another might modify the picture, but there is not yet any quantitative description of those effects.

THE FREDERIKS TRANSITION

The Frederiks transition provides a simple means for determining material parameters for nematic liquid crystals, provided that one can prepare well aligned single-crystal samples with strong anchoring of the director at the parallel plates defining the sample boundaries.

We have been able to prepare such samples of PBG nematics. Either homeotropic or parallel boundary conditions can be utilized to fix the director in a unique orientation at the parallel-plate sample surfaces. Homeotropic alignment occurs spontaneously for glass, fused silica or indium-tin oxide surfaces, presumably owing to hydrogen bonding of the PBG at the oxide surface. We have prepared parallel

boundary conditions by coating these oxide surfaces with a thin highly cross-linked polyethylene layer deposited by plasma polymerization of ethylene gas.¹⁰

For TMV, parallel orientation occurs spontaneously, and we have not thought of any way of preparing homeotropic samples.¹¹

The magnetic anisotropy of PBG is positive, so that it aligns parallel to a magnetic field.¹² For high-frequency electric fields (above *ca.* 100 kHz) the dielectric anisotropy is negative and electrohydrodynamic effects have disappeared, so the director aligns perpendicular to an electric field.¹³

The magnetic anisotropy of TMV is positive.¹⁴

In the following sections we describe the three main geometries for the Frederiks transition, together with our findings.

BEND GEOMETRY

With homeotropic boundary conditions and a magnetic field in the plane of the sample, or an electric field parallel to the director, the critical field for the Frederiks transition determines the bend elastic constant. The effective viscosity for this mode of distortion is very large, so the critical field is hard to find. This is the first kind of problem encountered, although it is one of inconvenience rather than fundamental difficulty. After exceeding the critical field by a small amount and creating a small distortion, one can change the field and see whether this distortion grows or shrinks with time, and thus bracket the critical-field value. By making a quantitative measurement of the amplitude of the distortion, for instance by monitoring the optical anisotropy of the sample, one sees that the response at a fixed field is an exponential relaxation in time toward the equilibrium state. By plotting the inverse of the time constant of this exponential against field, one can measure the critical field from the zero crossing and the effective viscosity from the slope of this line. This is slow work.

However, above twice the critical field a new and very fast distortion appears which is the second harmonic (mode two) of the fundamental distortion (mode one) occurring at the lower critical field.⁹ The effective viscosity for this mode of distortion is very small. Repeating the previous experiment near this critical field does not seem to be too difficult, since one can study the rapid response of mode two before mode one does anything (the ratio of speeds is of the order of a hundred or more). However, one discovers that the system does not respond exponentially even at rather small distortion amplitudes!¹⁵ This is the first real problem encountered.

The non-linear behaviour of this fast mode of distortion we have attributed to the influence of elongational flow viscosity, which appears as a second-order effect. The equation of motion for the angular distortion θ induced by the field can be written in the long-chain limit as

$$K_3 \frac{\partial^2 \theta}{\partial z^2} = (\eta_b + \alpha_1 \theta^2) \frac{\partial \theta}{\partial t}$$

for small amplitudes. Because the first-order viscosity, η_b , for this mode is very small while the coefficient of the non-linear term, α_1 , is of the order of a hundred times larger, the non-linear effects become important at very small amplitude, making the first-order viscosity hard to measure accurately. This is a new phenomenon that is not encountered in low-molecular-weight liquid crystals. It gives us a direct means of measuring the relative magnitude of the elongational flow viscosity.

If one knows the appropriate diamagnetic or dielectric anisotropy and one can measure the time dependence of the bend distortion accurately, one can determine K_3 and several viscosities using this geometry.

TWIST GEOMETRY

With parallel boundary conditions and the magnetic field parallel to the plane of the sample, we examined the twist Frederiks transition. Upon application of the field, a pattern of stripes appeared, oriented perpendicular to the undisturbed director, once again a new phenomenon.¹⁶ Exploring the field dependence of the stripe spacing and the time dependence of the pattern, we realized that this was a dynamic effect due to the large anisotropy of the viscosity of the material. For a suddenly applied field, above the critical field for the Frederiks transition, the periodic structure has a faster response time than a uniform twist response. There is a particular wavelength for which the stripes grow the fastest. That wavelength dominates the response, producing the stripes that are observed. This is a transient response, in the sense that eventually the stripes disappear, leaving the sample in a uniformly twisted state.

The uniform twist transition has viscosity γ_1 , which is very large. The stripe pattern involves coupled rotation and velocity fields; the magnetic field drives the director field of counter-rotating stripes, which in turn induces the velocity field. This combined set of fields has a much lower viscosity than γ_1 . Of course the stripe pattern has more internal elastic energy than the uniform twist distortion. It involves bend distortion as well as twist, and has in-plane components of curvature that are not involved in the uniform twist mode. This has two consequences. First, for a range of fields above the critical field for the uniform twist transition, the uniform mode may be the fastest. At some higher field the stripe pattern becomes faster. Secondly, the wavelength of the stripe pattern that maximizes the speed of response is kept long by the elastic energy, while the viscous factor favours a short wavelength. Therefore the observed wavelength is a compromise.

By measuring the wavelength of the observed stripe pattern as a function of applied field, one determines several things. The critical field for the ordinary twist Frederiks transition can still be determined, yielding K_2 . The behaviour above critical field gives an accurate value of K_2/K_3 , and two ratios of viscosities. Data for one preparation of TMV and details of the analysis are published elsewhere.¹¹

SPLAY GEOMETRY

With parallel boundary conditions and the field perpendicular to the plane of the sample, we attempted to study the splay Frederiks transition. Once again, on suddenly applying a large magnetic field, we observed the appearance of arrays of stripes, this time oriented obliquely to the original director orientation. The orientation and wavelength of the stripes depended on the field strength. Again, this was found to be a transient effect due to the anisotropy of the viscosity of the material. A theoretical analysis indicates how this effect can be used to determine ratios of material parameters. In this case, because of the complexity of the director and velocity fields, the analysis is rather complicated, and we have not found any simple way to extract data from the experiments. Nonetheless, if one knows some parameters, these measurements can be used to determine some others. Data on TMV and a detailed presentation of the theory for this instability and data analysis are presented elsewhere.¹⁷

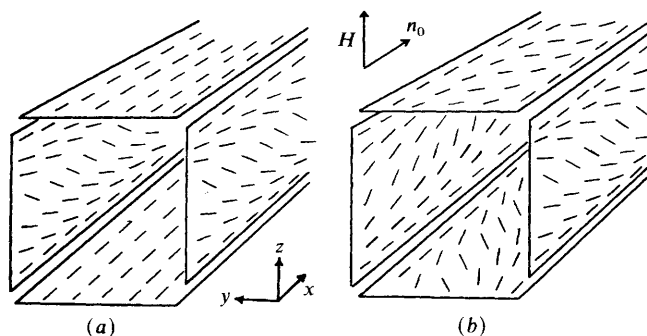


Fig. 1. Schematic representation of the replacement of a uniform splay structure in a planar sample (a) by a periodic twist pattern (b). This might also be referred to as a splay-compensated structure, since apparent splay in the plane of the sample is cancelled by another component of apparent splay perpendicular to that plane.

Attempting to avoid the stripes and determine the critical field for the splay Frederiks transition, we discovered another phenomenon. We could not achieve a uniform splay Frederiks transition in PBG. At the lowest field giving a response, we still observed stripes, parallel to the undisturbed director. This is a static effect. The explanation is that a new form of Frederiks transition replaces the uniform splay response. It is a periodic structure composed mostly of twist distortion (see fig. 1), which has a lower threshold field than the simple splay transition. It occurs if the ratio of splay to twist elastic constants is above 3.3. What is remarkable is that one can construct a stripe pattern that satisfies the boundary conditions that the distortion disappear at the surfaces, that couples to the external field, and that is composed of pure twist! The theory of this effect, predicting the critical field and the wavelength of the stripes, has been developed and has been published elsewhere.¹⁸ Neither the wavelength nor the critical field depends very strongly on the splay elastic constant, and both of those quantities are difficult to measure accurately. This leaves us in the position of having no simple means of measuring the splay elastic constant *via* the Frederiks transition.

LIGHT SCATTERING

Quasielastic depolarized Rayleigh scattering has been shown to be a useful way of determining elastic constants and viscosities of nematic liquid crystals.^{3,4} The PBG nematics are especially well suited to this technique because they have very low birefringence. This eliminates multiple scattering and makes the optical propagation equivalent to that in an isotropic medium. There is still enough birefringence to make the depolarized light scattering cross-section large enough for an adequate signal, using an argon laser at *ca.* 100 mW incident power.

With this technique one can study both the intensity of the scattered light and the time dependence of the fluctuations that scatter the light. The intensity is determined by the amplitude of the thermally excited director fluctuations which produce depolarized scattering. That amplitude depends only on the energy of the fluctuation, which is proportional to the appropriate elastic constant. One does not measure absolute intensities of scattered light, but in a situation in which one can measure a ratio of intensities or the dependence of intensity on some external variable, one can deduce information about the relative value of an elastic constant.

The time dependence is most efficiently studied by computing the autocorrelation function of the scattered light intensity in real time with a digital autocorrelator. The fluctuation modes in nematics are all overdamped, since their elastic energy is small and their viscosity is large. The autocorrelation function for a single mode is an exponential decay, the time constant of which depends on the ratio of a viscosity to an elastic constant.

We have studied two scattering geometries in samples with parallel boundary conditions.¹⁹ In the first the director is perpendicular to the scattering plane, with the incident polarization parallel to the director, and the scattered polarization parallel to the scattering plane. The plane of the sample is oriented so that the scattering wavevector is parallel to the glass plates. In the second geometry, everything is the same as in the first, except that the sample is rotated about an axis normal to its surface so that the director is parallel to the scattering wavevector.

The first geometry allows one to see scattering from a superposition of pure splay and pure twist modes. The ratio of the amplitudes of these modes depends on the ratio of twist and splay elastic constants, and their relaxation times depend on their effective viscosities. In the second geometry one sees scattering from a pure bend mode. Keeping the entire scattering geometry fixed and switching from the first sample orientation to the second, one can compare the amplitudes of the pure bend mode and the splay and twist modes. In this way one measures the ratio of the bend elastic constant to the others. The relaxation time of the pure bend mode determines another effective viscosity. These measurements are repeated at a number of scattering angles to confirm the correct angular dependence of the scattering intensities and relaxation times.

The results of these measurements are several ratios of elastic constants and viscosities. Combining these measurements with one of the critical fields for the Frederiks transition and a knowledge of the diamagnetic anisotropy leads to an absolute determination of a number of viscosities and the elastic constants of the sample. It is important to note that all the field and light scattering experiments can be performed on a single sealed sample of PBG or TMV, so that the data can be combined unambiguously. The birefringence and ultraviolet absorption spectrum²⁰ can also be measured on the same sample to determine its concentration and degree of orientational order.

DISCUSSION

We now have some quantitative data on the elastic and viscous properties of TMV^{11,17} and PBG¹⁹ nematics. We have deduced ratios of elastic constants and viscosities from measurements on the dynamic-stripe phenomena in one preparation of TMV. For PBG we have performed light-scattering experiments and some Frederiks-transition measurements on the same samples, which give compatible results.

The TMV is a carefully extracted preparation of monodisperse virus. From X-ray studies of the same preparation we roughly estimate its order parameter to be 0.9. Table 1 compares our measurements with hard-rod theory. For an order parameter of 0.8 the agreement would be remarkably good. The way these data are obtained is not *via* the most direct experiments, and the complex fitting procedures used for analysing the oblique stripes do not necessarily determine the parameters uniquely. Moreover, we only have ratios of various parameters, rather than absolute values. Nonetheless, the results are suggestive that the hard-rod model in the Onsager limit is not far from correct.

We have extensive data on one sample of PBG at a concentration just above the coexistence region, reported in table 1. The absolute values reported for various parameters are based on the published value for the diamagnetic anisotropy of PBG. The sample is obtained from the Sigma Chemical Co., which gives its degree of polymerization as 700, implying a length-to-diameter ratio of 70. The data could be consistent with either the hard-rod model or the semiflexible-chain limit. The concentration dependence and the molecular-weight dependence of the elastic constants and the viscosities will be crucial for distinguishing between these possibilities.

These experimental methods should also be useful for several other lyotropic polymer nematics, providing the opportunity to see if these systems are at all universal in their behaviour.

We thank Gerry Swislow for extensive assistance and instruction on computation. This research was supported in part by the U.S. National Science Foundation through grant no. DMR-8210477, and by the Martin Fisher School of Physics, Brandeis University.

¹ C. Robinson, *Tetrahedron*, 1961, **13**, 219.

² H. J. Deuling, in *Solid State Physics*, ed. H. Ehrenreich, F. Seitz, D. Turnbull and L. Liebert (Academic Press, New York, 1978), vol 14, pp. 77-107.

³ Orsay Group on Liquid Crystals, *J. Chem. Phys.*, 1969, **51**, 816.

⁴ Orsay Group on Liquid Crystals, *Phys. Rev. Lett.*, 1969, **22**, 1361.

⁵ L. Onsager, *Ann. N. Y. Acad. Sci.*, 1949, **51**, 627.

⁶ J. P. Straley, *Phys. Rev. A*, 1973, **8**, 2181.

⁷ N. Kuzuu and M. Doi, *J. Phys. Soc. Jpn*, 1983, **52**, 3486; 1984, **53**, 1031.

⁸ Sin-Doo Lee and Robert B. Meyer, in preparation.

⁹ R. B. Meyer, in *Polymer Liquid Crystals*, ed. A. Ciferri, W. R. Krigbaum and R. B. Meyer (Academic Press, New York, 1982), chap. 6.

¹⁰ V. G. Taratuta, G. M. Srajer and R. B. Meyer, *Mol. Cryst. Liq. Cryst.*, 1985, **116**, 245.

¹¹ S. Fraden, A. J. Hurd, R. B. Meyer, M. Cahoon and D. L. D. Caspar, *Proc. of the les Houches Workshop on Colloidal Crystals*, *J. Phys. (Paris)*, 1985, **46**, C3-85.

¹² N. S. Murthy, J. R. Knox and E. T. Samulski, *J. Chem. Phys.*, 1976, **65**, 4835.

¹³ F. Lonberg and R. B. Meyer, personal communication.

¹⁴ G. Maret, S. Fraden, M. Cahoon and D. L. D. Caspar, work in preparation.

¹⁵ F. Lonberg and R. B. Meyer, personal communication.

¹⁶ F. Lonberg, S. Fraden, A. J. Hurd and R. B. Meyer, *Phys. Rev. Lett.* 1984, **52**, 1903.

¹⁷ A. J. Hurd, S. Fraden, F. Lonberg and R. B. Meyer, *J. Phys. (Paris)*, 1985, **46**, 905.

¹⁸ F. Lonberg and R. B. Meyer, *Phys. Rev. Lett.*, 1985, **55**, 718.

¹⁹ V. G. Taratuta, A. J. Hurd and R. B. Meyer, *Phys. Rev. Lett.*, 1985, **55**, 246.

²⁰ V. G. Taratuta, personal communication.